Structural and Theoretical Studies of New Ruthenium-Amidato Complexes with Phenanthroline Ligands Containing H-Bonding Groups

Daniela Rais,[a] Ian R. Gould,[a] Ramón Vilar,*[a] Andrew J. P. White,[a] and David J. Williams[a]

Keywords: Chelates / Tridentate ligands / Ligand design / Ruthenium / pi interactions

The syntheses, characterization and coordination chemistry of two new 1,10-phenanthroline-based ligands are presented here. Crystallographic studies have shown that both molecules display hydrogen-bonding and π–π stacking interactions, generating interesting supramolecular assemblies in the solid state. The reactions of these ligands with $[RuCl_2(PPh_3)_3]$ have been performed and two new ruthenium-amidato complexes have been prepared. In both cases, the presence of a pyridyl group in the ligand backbone favours the deprotonation of one of the carboxyamido moieties leading to a tridentate coordination mode of the ligands. The structural characterization of one of the ruthenium complexes is also reported.

Introduction

Transition metal complexes featuring *N*-amidato [−NRC(=O)R′] ligands are relatively less common than those containing other *N*-based species such as amines (−NR_3) or amides (−NR_2). Nevertheless, increasing interest has recently been paid to *N*-amidato-containing systems due to their role as models for the interactions between metal centres and proteins.[1] To date, studies have largely focused on iron- and copper-amidato species[2,3] because of their biological relevance, and on cobalt systems due to their interesting catalytic properties.[4] Although some reports exist on the chemistry of *N*-amidato-ruthenium complexes, these have mainly dealt with pentaaminoruthenium amido species. Examples of compounds where the carboxyamido moiety is part of a more complex coordination environment are somewhat rare. However, the ability of ruthenium to participate in a wide range of catalytic and photochemical processes[5] coupled with the stability, ease of preparation and strong σ-donating properties of the amidato ligands have contributed to the renewed interest in these systems.[6,7] Synthetic and structural information on Ru^{II} and Ru^{III} complexes of deprotonated *N*-aryl-2-pyridinecarboxamide ligands has been reported by Bhattacharya[6] while Wright has investigated a series of Ru^{II} complexes of doubly deprotonated *N*,*N*′-bis(6-methyl-2-pyridinyl)-2,6-pyridinedicarboxamide.[7] In this context, the pendant pyridine moieties were found to interact with appropriately positioned ruthenium-bound molecules, thereby mimicking many metalloenzymes that influence the reactivity of bound substrates through interactions with the metal centre and functional groups present on the nearby protein backbone. The general ability of *N*-amidato ligands to stabilize metals in high coordination states was further confirmed by the generation and characterization of the Ru^{IV} species $[RuL_2]\cdot H_2O$ [H_2L = *N*,*N*′-bis(2-phenyl)-2,6-pyridinedicarboxamide].

As part of our interest in the chemistry of transition metal complexes that possess hydrogen bonding capabilities,[8] we have recently focused our efforts on the synthesis of 2,9-carboxyamido-substituted phenanthroline molecules. Metal complexes with hydrogen-bonding properties are of great interest due to their applications in the design of molecular receptors[9] as well as in the fields of crystal engineering[10] and supramolecular catalysis.[11] Herein we report the synthesis and characterization of two phenanthroline-carboxamide ligands (H_2L1 and L2 in Scheme 1) and the products resulting from their reactions with $[RuCl_2(PPh_3)_3]$.

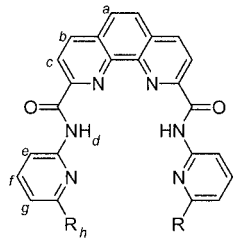

R = NH_2, **L1**; H, **L2**

Scheme 1

[a] Department of Chemistry, Imperial College London, South Kensington, London SW7 2AY, UK
Fax: (internat.) + 44-20-7594-5804
E-mail: r.vilar@ic.ac.uk

Results and Discussion

Synthesis of Phenanthroline-Based Ligands H_2L1 and L2

The two molecules *N*,*N*′-bis(2-amino-6-pyridyl)-1,10-phenanthroline-2,9-carboxamide (in its protonated form, H_2L1) and *N*,*N*′-bis(2-pyridyl)-1,10-phenanthroline-2,9-carboxyamide (L2) (Scheme 1) were obtained in good yields (60 and 91 %, respectively) by reaction of 1,10-phenanthroline-2,9-dicarbonyl chloride (prepared from neocuproine by previously reported methods[12]) with the corresponding amine.

The new compounds were characterized by analytical and spectroscopic means. The IR spectra of the two species showed broad bands centred at $\tilde{\nu}$ = 3326 and 3333 cm^{-1} for H_2L1 and L2, respectively, which were assigned to the ν(NH) band of the carboxyamido groups. In the ^1H NMR spectra, the CO−N*H* proton was found to resonate as a singlet at δ = 10.33 and 11.17 ppm for H_2L1 and L2, respectively. A single set of resonances was observed for the two halves of the molecules indicating their equivalence on the NMR time scale.

The structural features of the newly synthesized molecules were elucidated by performing single-crystal X-ray analyses. It should be noted that attempts to crystallise the protonated H_2L1 species were not successful; instead, a very small number of single crystals of the deprotonated form of this compound (i.e. L1) were obtained and structurally characterised. This suggests that, although the bulk of the material is isolated as the diprotonated form (see below) a small amount of the neutral form is also present (which forms single crystals).

In the solid state L1 has a nonplanar hemi-helical conformation, there being a significant twist of the phenanthroline unit with rings **B** and **D** inclined by approximately 9° (see Figure 1). One of the amide groups [associated with N(16)] is held in an almost co-planar arrangement with its adjacent phenanthroline pyridyl ring **B** by an intramolecular N−H···N hydrogen-bond (**f** in Figure 1); rings **A** and **B** are inclined by approximately 3°. By contrast, the other amide group is rotated substantially out of plane, the torsional twists about C(11)−C(24) and N(25)−C(26) being approximately 24 and 33°, respectively [cf. ca. 4 and 3° about C(2)−C(15) and N(16)−C(17)]. However, these rotations are in opposite senses such that rings **D** and **E** which are inclined by approximately 8°, are in a stepped relationship to each other. This second amide group is not intramolecularly hydrogen-bonded to its adjacent phenanthroline pyridyl ring **D** (N···H 2.40 Å), entering instead into intermolecular hydrogen-bonding with the carbonyl oxygen atom of the "first" amide of a centrosymmetrically related counterpart (**b** in Figure 2). There is also an intermolecular N−H···N hydrogen bond between the N(23) terminal amino group of one molecule and the pyridyl nitrogen atom N(18) of another across an independent inversion centre (**a** in Figure 2). These interactions, combined with π−π stacking interactions **c** and **d**, create a continuous "staircase-like" chain of alternating hemi-helices that progresses along the crystallographic *a* direction. Adjacent chains are cross-linked by N−H···O hydrogen bonds between the other terminal amide group N(32) in one chain and the carbonyl oxygen O(24) of the next [N···O, H···O 3.00, 2.10 Å; N−H···O 175°].

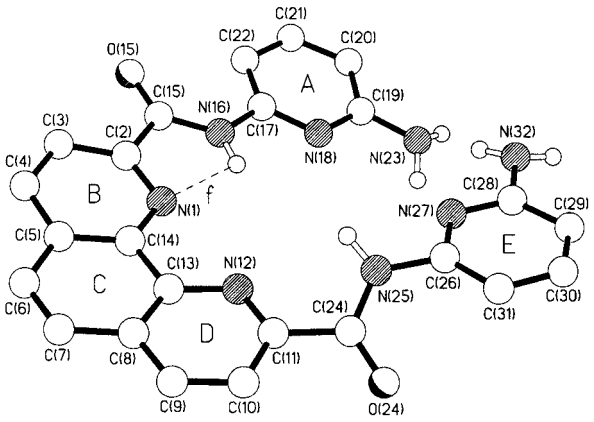

Figure 1. Molecular structure of L1; the intramolecular N−H···N hydrogen bond **f** has N···N, H···N 2.69, 2.24 Å and N−H···N 111°; the nonbonded N(23)···N(32) separation is 3.47 Å

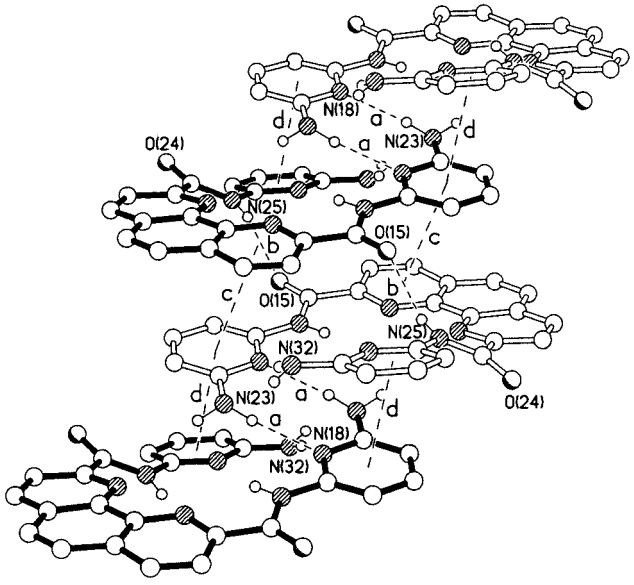

Figure 2. Part of one of the continuous "staircases" in the solid-state structure of L1; the hydrogen bonding geometries [N···X, H···X (Å), N−H···X (°)] are **a** 3.08, 2.18, 174; **b** 2.97, 2.16, 149; the centroid···centroid separations are **c** 3.58 Å and **d** 3.67 Å, the interacting rings being inclined by 3 and 19°, respectively

The related molecule L2 has a similar conformation but with a smaller distortion of the central phenanthroline ring system-rings **B** and **D** being inclined by approximately 4° (see Figure 3). Rings **A** and **B** are inclined by approximately 9°, and **D** and **E** by approximately 35°. The two amide groups, however, are both essentially co-planar with, and intramolecularly N−H···N hydrogen bonded to (**f** and **g** in Figure 3), their adjacent phenanthroline pyridyl rings; the torsional twists about C(11)−C(23) and C(2)−C(15) are

approximately 2 and 11°, respectively. The molecules pack to form continuous stacks along the crystallographic *a* direction (Figure 4), there being a parallel π−π stacking interaction between ring **B** of one molecule and its centrosymmetrically related counterpart in another (centroid···centroid and mean interplanar separations of 3.87 and 3.57 Å, respectively). The other stacking interaction is more unusual, and involves an orthogonal approach of the amide N($p\pi$) orbital of N(24) in one molecule to ring **C** of another and *vice versa* across an independent inversion centre; the N···centroid distance **b** is 3.42 Å and the N···centroid vector is inclined by approximately 86° to the {C(23)−N(24)−C(25)} plane.

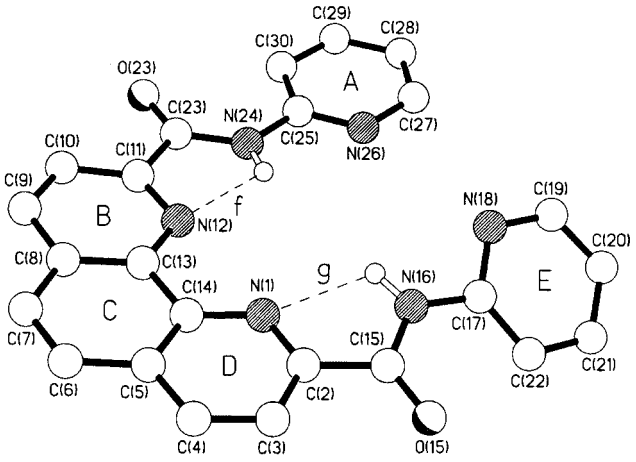

Figure 3. Molecular structure of L2; the intramolecular N−H···N hydrogen bonding geometries [N···N, H···N (Å), N−H···N (°)] are **f** 2.65, 2.16, 114; **g** 2.67, 2.21, 111

Synthesis of $[RuCl_2(L1)(PPh_3)]$ (1)

Reaction of $[RuCl_2(PPh_3)_3]$ with H_2L1 in a DMF/toluene solvent mixture led to isolation of complex $[RuCl_2(L1)(PPh_3)]$ (**1**) in 84% yield (Scheme 2). The initially dark brown suspension was refluxed for 4 hours under a N_2 atmosphere, turning dark purple after approximately 30 min. Filtration of the suspension yielded **1** as a dark purple powder.

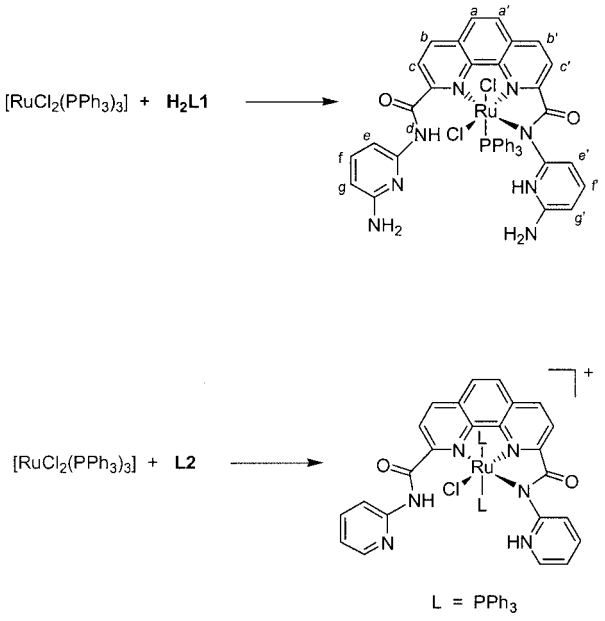

Scheme 2

The new compound was found to be air stable and could be characterized by means of IR, $^{31}P\{^1H\}$ and ^1H NMR spectroscopy, FAB^+ mass spectrometry and elemental analyses. The formulation based on the analytical and spectroscopic data was further confirmed by a single-crystal X-ray structural determination. Suitable crystals were obtained by layering diethyl ether onto a solution of **1** in DMF.

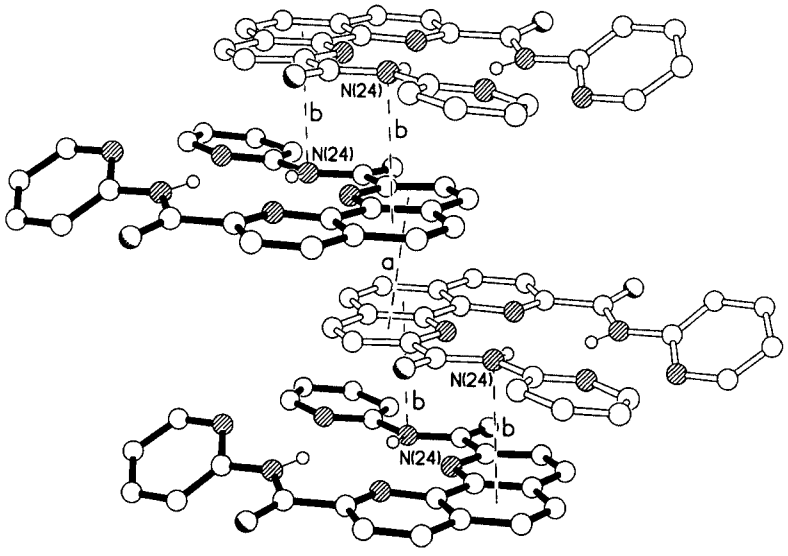

Figure 4. Part of one of the continuous stacks of molecules in the structure of L2; the centroid···centroid separation **a** is 3.87 Å and the N···centroid distance **b** is 3.42 A

The X-ray analysis showed L1 to be coordinated to the ruthenium centre in an asymmetric tridentate fashion, forming two coordinative Ru−N bonds with the phenanthroline nitrogen atoms and a Ru−N amidato bond with a deprotonated carboxyamido unit, the amido proton having been transferred to N(18) of the adjacent aminopyridine ring (Figure 5).

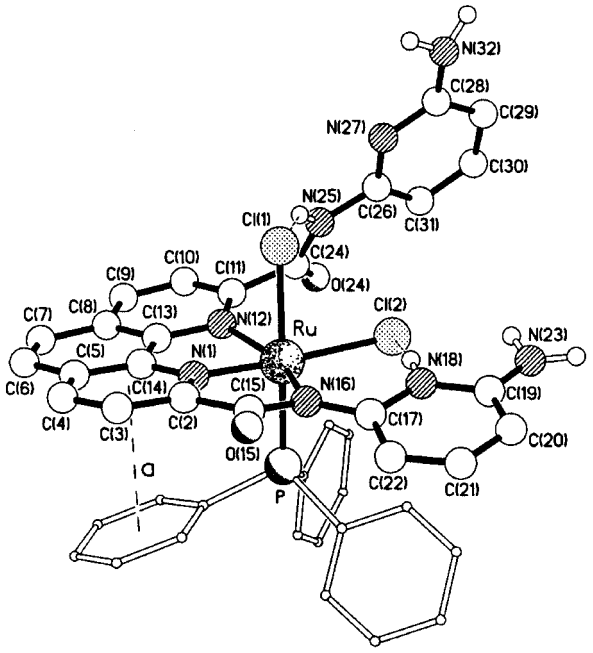

Figure 5. Molecular structure of $[RuCl_2(L1)(PPh_3)]$ (**1**); the centroid···centroid separation **a** is 3.47 Å and the rings are inclined by approximately 16°

The coordinated amido arm of the ligand lies within the equatorial coordination plane, the torsional twists about C(2)−C(15) and N(16)−C(17) being approximately 5 and 17°, respectively, a geometry that facilitates an intramolecular N−H···Cl hydrogen bond from the pyridinium nitrogen N(18) to the equatorially coordinated chloride Cl(2) [N···Cl, H···Cl 2.99, 2.12 Å; N−H···Cl 163°]. By contrast the other arm is rotated substantially out of plane−the torsional twists about C(11)−C(24) and N(25)−C(26) are approximately 54 and 12°, respectively, thereby directing the amide N−H group towards the axially coordinated chloride Cl(1); here the N−H···Cl hydrogen bond is noticeably weaker [N···Cl, H···Cl 3.36, 2.55 Å; N−H···Cl 150°]. The phenanthroline unit has a warped geometry very similar to that seen in the free ligand, the two pyridyl rings being inclined by approximately 10°. The geometry at ruthenium is distorted octahedral with *cis* angles in the range 77.4(2) to 93.0(1)°, the most acute angles being associated with the five-membered chelate rings (see Table 1 and Table 2) which are coplanar to within 0.06 Å. There is a substantial distortion of the *trans* N(12)−Ru−N(16) angle [156.8(2)°] which is a consequence of the geometrical constraints of the chelating ligand. The Ru−N(1) bond [1.951(5) Å] is, as expected, significantly shorter than those to N(12) [2.163(5) Å] and N(16) [2.156(5) Å]. The Ru−Cl(1) bond [2.469(2) Å], *trans* to P, is noticeably shorter than that to Cl(2) [2.493(1) Å] *trans* to N(1). It is interesting to note that the asymmetric chelating mode of the ligand is also reflected in an asymmetric pattern of bonding within the phenanthroline ring system−for example, though the N(1)−C(2) [1.332(8) Å] and N(1)−C(14) [1.340(8) Å] bond lengths are the same, those between N(12)−C(13) [1.392(7) Å] and N(12)−C(11) [1.329(8) Å] differ significantly. A similar (but expected) asymmetry is seen between the two amide groups, with the C−N bond in the deprotonated amide [C(15)−N(16) 1.380(8) Å] being significantly elongated compared with its counterpart [C(24)−N(25) 1.327(9) Å]. This asymmetry is also observed in the solution ^{1}H NMR spectra and in the solid-state infrared spectra (vide infra). The orientation of the triphenylphosphane is to some extent influenced by an intramolecular π−π stacking interaction (**a** in Figure 5) between one of the phosphane phenyl rings and the N(1) pyridyl ring of the phenanthroline. The only inter complex interaction of note is a π−π stacking interaction between the N(12) containing pyridyl ring of the phenanthroline unit in one molecule and the N(18) aminopyridinium ring of another, the centroid···centroid separation is 3.65 Å and the rings are inclined by approximately 14°. The only other noteworthy intermolecular interactions are N−H···O hydrogen bonds between the terminal amine groups and included dimethylformamide (DMF) solvent molecules. The N(32) amino group is involved in two N−H···O hydrogen bonds to the oxygen atoms of two centrosymmetrically related DMF molecules, linking pairs of complexes [N···O, H···O (Å), N−H···O (°); 2.95, 2.07, 167; 3.02, 2.13, 170]. The other terminal amino group [N(23)] forms a single hydrogen bond to an independent DMF solvent molecule [N···O, H···O 2.69, 1.81 Å, N−H···O 165°].

Table 1. Selected bond lengths (Å) for L1 and **1**

	L1	1		L1	1
Ru−Cl(1)	−	2.469(2)	Ru−Cl(2)	−	2.4929(14)
Ru−P	−	2.294(2)	Ru−N(1)	−	1.951(5)
Ru−N(12)	−	2.163(5)	Ru−N(16)	−	2.156(5)
N(1)−C(2)	1.331(3)	1.332(8)	N(1)−C(14)	1.357(3)	1.340(8)
C(2)−C(15)	1.502(3)	1.491(9)	C(11)−N(12)	1.327(3)	1.329(8)
C(11)−C(24)	1.510(3)	1.521(9)	N(12)−C(13)	1.362(3)	1.392(7)
C(13)−C(14)	1.454(3)	1.417(8)	C(15)−O(15)	1.226(3)	1.229(8)
C(15)−N(16)	1.353(3)	1.380(8)	C(24)−O(24)	1.223(3)	1.241(8)
C(24)−N(25)	1.348(3)	1.327(9)			

Table 2. Selected bond angles (°) for **1**

Cl(1)−Ru−Cl(2)	88.52(5)	P−Ru−Cl(1)	179.19(5)
P−Ru−Cl(2)	92.26(6)	N(1)−Ru−N(16)	77.4(2)
N(1)−Ru−N(12)	79.7(2)	N(16)−Ru−N(12)	156.8(2)
N(1)−Ru−P	91.4(2)	N(16)−Ru−P	91.0(2)
N(12)−Ru−P	92.97(14)	N(1)−Ru−Cl(1)	87.8(2)
N(16)−Ru−Cl(1)	88.60(14)	N(12)−Ru−Cl(1)	87.08(14)
N(1)−Ru−Cl(2)	176.3(2)	N(16)−Ru−Cl(2)	102.44(14)
N(12)−Ru−Cl(2)	100.26(13)		

The ligand's asymmetric coordination was reflected in the IR spectrum of complex **1** which showed two different carbonyl absorptions: the one at $\tilde{\nu}$ = 1683 cm^{-1} was assigned to the CO stretching of the noncoordinated carboxamide while the one at $\tilde{\nu}$ = 1638 cm^{-1} was attributed to the CO stretching of the *N*-coordinated amidato group, in agreement with values reported in the literature for analogous *N*-bound amidato ligands (see the calculations section for a discussion of these values). Several bands were observed in the N−H bond stretching region but their assignment was found to be problematic given the numerous N−H groups present in the molecule; only after quantum mechanical calculations were performed it was possible to assign these values (see calculations section). The $^{31}P\{^{1}H\}$ NMR spectrum showed a singlet at δ = 45.0 ppm, shifted downfield with respect to the starting material ($[RuCl_2(PPh_3)_3]$, 42.0 ppm). The ^{1}H NMR spectrum of **1** in $[D_6]$DMF displayed an extremely complicated pattern in the aromatic region, consistent with the asymmetric coordination of the ligand to the ruthenium centre (as shown in the solid-state structure). The N−H group of the noncoordinated carboxamide was observed as a singlet at δ = 10.58 ppm while a signal at δ = 13.74 ppm was assigned to the pyridinium proton.

Synthesis of *trans*-[RuCl(L2)(PPh_3)$_2$]Cl (*trans*-2)

By analogy with the synthesis of **1**, the reaction of $[RuCl_2(PPh_3)_3]$ with one equivalent of L2 was investigated. However, instead of the expected $[RuCl_2(L2)(PPh_3)]$ a complex with formula $[RuCl(L2)(PPh_3)_2]Cl$ was obtained (Scheme 2). Upon mixing the reactants in DMF/toluene, a deep purple solution was immediately formed. The mixture was stirred at room temperature for 2 hours yielding a dark purple precipitate. The $^{31}P\{^{1}H\}$ NMR spectrum of the solid in $[D_2]$-dichloromethane showed two doublets at δ = 49.7 and 39.6 ppm ($J_{P,P}$ = 36.0 Hz), indicating the presence of two nonequivalent phosphane ligands in this species. However, during the course of the NMR studies it was observed that the compound was not stable since a dark purple solid precipitated few minutes after the $[D_2]$-dichloromethane solution (originally highly coloured and perfectly clear) had been prepared. After 1 hour the entire soluble compound had been transformed into the dichloromethane-insoluble product and no $^{31}P\{^{1}H\}$ NMR signal could be detected in the supernatant solution. The resulting purple solid was isolated by filtration and analyzed by $^{31}P\{^{1}H\}$ NMR and IR spectroscopy, FAB^+ mass spectrometry and elemental analyses. On the basis of the spectroscopic and analytical data, the compound was formulated as *trans*-$[RuCl(L2)(PPh_3)_2]Cl$ (*trans*-**2**).

The $^{31}P\{^{1}H\}$ NMR spectrum of *trans*-**2** in $[D_6]$DMF showed the presence of a singlet resonance at δ = 25.5 ppm, in contrast to the value of 43.0 ppm observed for **1**. The chemical shift of 25.5 ppm is consistent with previously reported data for ruthenium complexes where two triphenylphosphane ligands are *trans* to each other (and *cis* to chlorides and chelating *N*-ligands).[13] The formulation of *trans*-**2** was further supported by FAB^+ mass spectrometry which showed a molecular ion peak a.m.u. at 1081 corresponding to $[RuCl(L2)(PPh_3)_2]^+$. The IR spectrum of *trans*-**2** was also consistent with the proposed formulation showing two bands at $\tilde{\nu}$ = 1690 and 1648 cm^{-1} that were assigned to the carbonyl stretching modes of a nondeprotonated amide (i.e. the noncoordinated one) and a coordinated amidato group, respectively, on the basis of quantum-mechanical calculations (see below). The asymmetric coordination of ligand L2 in complex *trans*-**2** found support in the ^{1}H NMR spectrum of the compound, which showed a very complicated pattern for the protons on the phenanthroline and the pyridine moieties and the presence of two different CO-N*H* resonances (whose values were consistent with that of a noncoordinated carboxamide and a protonated pyridine group). Elemental analyses agreed with the proposed formulation.

The identity of the solid obtained during the first stage of the reaction between L2 and $[RuCl_2(PPh_3)_3]$ is uncertain. However, the available spectroscopic and analytical data [$^{31}P\{^{1}H\}$ NMR spectrum, elemental analyses and FAB^+ mass spectrum] are compatible with a formulation of the purple powder as *cis*-$[RuCl(L2)(PPh_3)_2]Cl$ (*cis*-**2**). It is reasonable to propose that compound *cis*-**2** is formed as the kinetic product of the reaction and isolated as a solid due to its insolubility in the reaction medium. However, once in either dichloromethane or DMF solution, it rapidly converts to its thermodynamically more stable isomer *trans*-**2**.

Quantum-Mechanical Calculations

To gain a better understanding of the nature of the ruthenium-amidato complexes and be able to rationalize some of their spectroscopic and structural parameters, a quantum mechanical study of complexes **1** and **2** was carried out. It was also of interest to compare the relative energy of the *cis* and *trans* isomers of complex **2**.

Selected structural parameters for compounds **1** and *trans*-**2** are reported in Table 3 and Table 4. It can be seen that the calculated structure of **1** is in reasonably good agreement with that determined crystallographically (see Tables 1 and 2). The calculated molecular structure of *trans*-**2** is shown in Figure 6, the bond lengths and angles around the ruthenium centres being in good agreement with the crystallographic data of **1**. As would be expected, the largest difference between the calculated structures of **1** and *trans*-**2** is observed in the bond length between the Ru and the P atoms due to the different *trans* influence of the chloride (in **1**) and the phosphane (in *trans*-**2**).

Minima have been obtained for both *cis*-**2** and *trans*-**2** and, as expected on steric grounds, the *trans* isomer is calculated to be more stable than the *cis* isomer by ca. 30 kcal mol^{-1}. These findings sustain our hypothesis that *cis*-**2** may indeed be the kinetic product of the reaction of L2 and $[RuCl_2(PPh_3)_3]$ which, however, easily coverts to its thermodynamically more stable isomer *trans*-**2**.

Inspection of the vibrational modes of **1** shows good correlation with the experimental data. There are two distinct carbonyl absorptions: one at $\tilde{\nu}$ = 1661 cm^{-1}, corresponding to the CO stretch of the noncoordinated carboxamide (cf. experimental $\tilde{\nu}$ = 1683 cm^{-1}), while the CO of the

Table 3. (a) Selected bond lengths (Å) for **1** and *trans*-**2**

	1	*trans*-**2**		**1**	*trans*-**2**
Ru−Cl(1)	2.473	−	Ru−Cl(2)	2.617	−
Ru−P	2.369	2.480	Ru−N(1)	1.964	1.980
Ru−N(12)	2.211	2.185	Ru−N(16)	2.189	2.191
N(1)−C(2)	1.340	1.338	N(1)−C(14)	1.359	1.359
C(2)−C(15)	1.484	1.488	C(11)−N(12)	1.347	1.347
C(11)−C(24)	1.515	1.510	N(12)−C(13)	1.389	1.385
C(13)−C(14)	1.422	1.420	C(15)−O(15)	1.251	1.248
C(15)−N(16)	1.390	1.403	C(24)−O(24)	1.254	1.249
C(24)−N(25)	1.354	1.357			

Table 4. Selected bond angles (°) for **1** and *trans*-**2**

	1	*trans*-**2**		**1**	*trans*-**2**
Cl(1)−Ru−Cl(2)	94.10	−	P−Ru−Cl(1)	176.40	−
P−Ru−Cl(2)	82.30	82.06	N(1)−Ru−N(16)	77.27	77.55
N(1)−Ru−N(12)	79.33	79.07	N(16)−Ru−N(12)	154.90	156.60
N(1)−Ru−P	93.23	90.80	N(16)−Ru−P	96.80	90.40
N(12)−Ru−P	95.80	90.73	N(1)−Ru−Cl(1)	90.40	−
N(16)−Ru−Cl(1)	94.46	−	N(12)−Ru−Cl(1)	85.22	−
N(1)−Ru−Cl(2)	175.52	172.83	N(16)−Ru−Cl(2)	102.84	103.12
N(12)−Ru−Cl(2)	101.21	103.13			

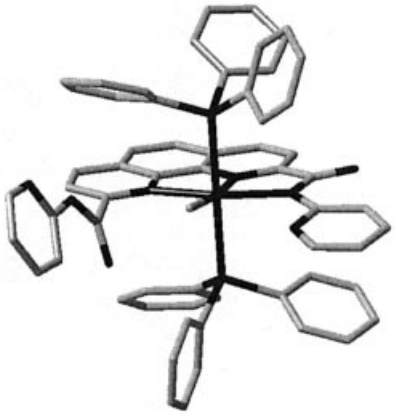

Figure 6. Calculated molecular structure of $[RuCl(L2)(PPh_3)_2]Cl$ (**2**)

N−coordinated amidato group is identified by two bands at $\tilde{\nu}$ = 1651 and 1648 cm^{-1} (cf experimental $\tilde{\nu}$ = 1638 cm^{-1}). We have also identified a very distinct N−H stretch at $\tilde{\nu}$ = 3062 cm^{-1} (cf. experimental $\tilde{\nu}$ = 3050 cm^{-1}), associated with the protonated pyridine group which forms a hydrogen bond with Cl(2). A second strong stretching frequency at $\tilde{\nu}$ = 3244 cm^{-1} (cf. experimental $\tilde{\nu}$ = 3234 cm^{-1}), is associated with the N−H bond of the noncoordinated amide [i.e. N(25)−H] which forms a hydrogen bond to the apical Cl(1) chloride.

We observe the same vibrational progression in *trans*-**2** with the carboxamide CO stretch at $\tilde{\nu}$ = 1669 cm^{-1}, the amidato CO at $\tilde{\nu}$ = 1657 cm^{-1}, the N−H···Cl (from the protonated pyridine group) at $\tilde{\nu}$ = 3048 cm^{-1} and the N−H (from the noncoordinated amide) at $\tilde{\nu}$ = 3442 cm^{-1} (cf. experimental $\tilde{\nu}$ = 1683, 1648, 3048 and 3342 cm^{-1}, respectively). It is worth noting that the frequency associated with the N−H of the noncoordinated amide in *trans*-**2** (calculated value of $\tilde{\nu}$ = 3442 cm^{-1}) is larger than the frequency associated with the same moiety in compound **1** (calculated value of $\tilde{\nu}$ = 3244 cm^{-1}). This is not surprising since in **1** the N−H group of the noncoordinated amide is hydrogen-bonding to the apical chloride of the complex weakening the bond and hence lowering the stretching frequency.

Conclusions

Two new phenanthroline-carboxamide ligands have been prepared and fully characterised. Crystallographic studies have shown that both ligands display various supramolecular interactions in the solid state. Particularly interesting are those observed for L1 where a combination of H-bonding and π−π stacking interactions create a continuous "staircase-like" chain of alternating hemi-helices. The reactions of H_2L1 and L2 with $[RuCl_2(PPh_3)_3]$ result in the formation of two different type of complexes. While the reaction with H_2L1 yields $[RuCl_2(L1)(PPh_3)]$ (**1**), the reaction with L2 leads to formation of *trans*-$[RuCl(L2)(PPh_3)_2]Cl$ (*trans*-**2**). The difference in reactivity could be due to the fact that, while **2** is formed from the neutral ligand L2, **1** is prepared using the hydrochloride salt of L1 (i.e. H_2L1) and hence there is a different concentration of chloride anions in the reaction mixtures. It is also possible that the difference could result from the sterically more demanding nature of L1 (due to the presence of the amino group in position 6 of the pyridine ring) in comparison to L2. However, in both cases the deprotonation of one of the carboxyamido moieties leads to the formation of a ruthenium-amidato bond and consequent tridentate coordination mode of the ligands. Structural characterisation of complex **1** has confirmed this coordination mode. On the basis of our results, we propose that the generation of complex *trans*-**2** takes place through a process in which the corresponding *cis* isomer (presumably kinetically favoured) is likely to be initially formed. However, this isomer rapidly rearranges to the thermodynamically more stable *trans*-**2** once it is dissolved in an appropriate solvent. Quantum mechanical calculations indicate that *trans*-**2** is indeed thermodynamically more stable than *cis*-**2** supporting the experimental observations. Furthermore, these calculations have allowed us to make a detailed assignment of some of the stretching frequencies observed in the IR spectrum of the new complexes. The experimental and calculated structural parameters for compound **1** are in good agreement.

Experimental Section

General: All manipulations were carried out in an atmosphere of purified and dry N_2 using standard Schlenk line techniques unless otherwise stated. Solvents were dried from the appropriate drying agent, degassed and stored under N_2. All commercially available solid starting materials were not further purified. ^1H and $^{31}P\{^1H\}$

NMR spectra were recorded on a JEOL-EX270 spectrometer (δ = 270.17 and 109.38 MHz, respectively) with TMS and H_3PO_4, respectively, as internal references. IR spectra were recorded on Research Series FT-IR using KBr disks in the range 4000−500 cm^{-1}.

Protonated Form of *N,N′*-Bis(2-amino-6-pyridyl)-1,10-phenanthroline-2,9-carboxamide (H_2L1): A solution of 2,6-diaminopyridine (2.5 g, 22.8 mmol) in CH_2Cl_2 (50 cm^3) was added dropwise to a suspension of 1,10-phenanthroline-2,9-dicarbonyl chloride (1.21 g, 3.8 mmol) in CH_2Cl_2 (50 cm^3) over 1 hour. A pale yellow precipitate formed immediately. The suspension was stirred overnight at room temperature. The mixture was filtered and the resulting precipitate washed with ethanol to extract excess amine, yielding H_2L1 as a pale yellow solid. Yield 1.2 g (60%). $C_{24}H_{18}N_8O_2$·2HCl (523): calcd. C 55.07, H 3.82, N 21.42; found C 55.02, H 3.86, N 21.51. IR (KBr): $\tilde{\nu}$ = 3443 (s), 3399 (m) (NH_2), 3326 (s) (CO−*NH*), 1680 (vs) (CO), 1644 (m), 1605 (m), 1580 (m) (C=N). ^{1}H NMR ([D_6]DMSO): δ = 10.33 (s, CO−N*H*, 1 H), 8.83 (d, H_b, $^3J_{H,H}$ = 8.4 Hz, 1 H), 8.57 (d, H_c, $^3J_{H,H}$ = 8.4 Hz, 1 H), 8.25 (s, H_a, 1 H), 7.53−7.40 (m, H_e, H_f, 2 H), 6.35 (d, H_g, $^3J_{H,H}$ = 5.7 Hz, 1 H), 5.82 (s, NH_2, 2 H) (see Scheme 1 for assignments). FAB$^+$−MS: *m*/*z* = 451 [M − 2HCl]$^+$

***N,N′*-Bis(2-pyridyl)-1,10-phenanthroline-2,9-carboxamide (L2):** A solution of 2-aminopyridine (1.75 g, 18.64 mmol) in CH_2Cl_2 (20 cm^3) was added dropwise to a suspension of 1,10-phenanthroline-2,9-dicarbonyl chloride (1.43 g, 4.7 mmol) in CH_2Cl_2 (20 cm^3). A dark brown solution formed immediately and was stirred at room temperature overnight yielding a white precipitate. The suspension was filtered and the precipitate washed with EtOH (3×10 cm^3) to extract the excess amine, yielding L2 as an off-white powder. Yield: 1.06 g, (91%). $C_{24}H_{16}N_6O_2$ (420): calcd. C 68.57, H 3.81, N 20.0; found C 68.48, H 3.95, N 19.73. IR (nujol): $\tilde{\nu}$ = 3353 (w), 3333 (w) (CO−*NH*), 1690 (vs) (C=O), 1587 (w), 1574 (w) (C=N). ^{1}H NMR ($CDCl_3$): δ = 11.17 (s, CO−*NH*, 1 H), 8.64 (d, H_b, $^3J_{H,H}$ = 8.4 Hz, 1 H), 8.49−8.43 (m, H_c, H_e, H_h, 3 H), 7.95 (s, H_a, 1 H), 7.81 (t, H_f, $^3J_{H,H}$ = 8.6 Hz, 1 H), 7.16−7.13 (m, broad, H_g, 1 H) (see Scheme 1 for assignments). FAB$^+$−MS: *m*/*z* = 421 MH^+.

[$RuCl_2$(L1)(PPh_3)] (1): Solid [$RuCl_2(PPh_3)_3$] (0.72 g, 0.75 mmol) was added to a solution of H_2L1 (0.34 g, 0.66 mmol) in a mixture of DMF/toluene (in a 1:5 ratio). The brown mixture was refluxed for 4 hours turning purple after ca 30 minutes then stirred overnight at room temperature. The suspension was then filtered and the precipitate washed several times with toluene and diethyl ether yielding **1** as a dark purple solid. Yield: 0.493 g, (84%). $C_{42}H_{33}Cl_2N_8O_2PRu$ (884.1): calcd. C 57.01, H 3.73, N 12.67; found calcd. C 57.07, H 3.68, N 12.67. IR (KBr): $\tilde{\nu}$ = 3234 (m) (CO−*NH*, noncoordinated carboxamide), 3050 (m) (py*H*), 1683 (s) (CO, noncoordinated carboxamide), 1638 (vs) (CO, *N*−bound amidato group). ^{1}H NMR ([D_6]DMF): 13.74 (s, py*H*, 1 H), 10.58 (s, CO−*NH*, 1 H), 8.41 (d, $H_{b'}$, $^3J_{H,H}$ = 8.3 Hz, 1 H), 7.97 (d, $H_{c'}$, $^3J_{H,H}$ = 8.3 Hz, 1 H), 7.94−7.81 (m, H_e, $H_{e'}$, H_g, $H_{g'}$ 4 H), 7.79 (s, H_a and $H_{a'}$, 2 H), 7.63 (d, H_b, $^3J_{H,H}$ = 8.3 Hz, 1 H), 7.46 (d, H_c, $^3J_{H,H}$ = 8.3 Hz, 1 H), 7.37 (t, H_f, $^3J_{H,H}$ = 8.3 Hz, 1 H), 7.25 (t, H_f, $^3J_{H,H}$ = 8.0 Hz, 1 H), 6.93−6.71 (m, PPh_3, 20 H) (see Scheme 2 for assignment); ^{31}P{^{1}H} NMR ([D_6]DMF): δ = 45.0; FAB$^+$−MS: *m*/*z* = 885 [M]$^+$, 849 [Ru(L1)(PPh_3)Cl]$^+$, 813 [Ru(L1)(PPh_3)]$^+$, 550 [Ru(L1)]$^+$.

***trans*-[RuCl(L2)(PPh_3)$_2$]Cl (*trans*-2):** Solid [$RuCl_2(PPh_3)_3$] (0.51 g, 0.53 mmol) was added to a solution of **L2** (0.22 g, 0.53 mmol) in a mixture of DMF/toluene (in a 1:5 ratio). A dark violet solution formed immediately and after few minutes a dark purple precipitate started forming. The suspension was stirred for 2 hours and the solid formed filtered off. The precipitate was washed several times with toluene and diethyl ether. The solid was re-dissolved in CH_2Cl_2 yielding a purple solution. After a few minutes the solution

Table 5. Crystal data, data collection and refinement parameters for compounds $\mathbf{L_1}$, $\mathbf{L_2}$ and **1**[a]

	L1	**L2**	**1**
Empirical formula	$C_{24}H_{18}N_8O_2$	$C_{24}H_{16}N_6O_2$	$C_{42}H_{33}N_8O_2PCl_2Ru$
Solvent	−	−	2 Me_2NCHO
Molecular mass	450.5	420.4	1030.9
Colour, habit	yellow needles	colourless prisms	very dark claret rhombs
Crystal size / mm	0.50 × 0.08 × 0.07	0.93 × 0.27 × 0.17	0.50 × 0.33 × 0.30
Temperature / K	293	293	183
Crystal system	monoclinic	orthorhombic	monoclinic
Space group	$P2_1/c$ (no. 14)	*Pbca* (no. 61)	$P2_1/n$ (no. 14)
a (Å)	9.176(1)	7.433(1)	12.922(1)
b (Å)	14.203(1)	23.051(3)	17.280(3)
c (Å)	16.309(1)	23.356(3)	21.165(4)
β / deg	102.53(1)	−	98.77(2)
V / Å^3	2075.0(3)	4001.8(9)	4671(1)
Z	4	8	4
D_c / g cm^{-3}	1.442	1.396	1.466
Radiation used	Cu-K_α	Cu-K_α	Cu-K_α[b]
μ / mm^{-1}	0.802	0.762	4.55
θ range / deg	4.2−60.0	3.8−60.0	3.3−60.0
No. of unique reflections measured	3076	2970	6893
observed, $\|F_o\| > 4\sigma(\|F_o\|)$	2423	2039	5022
Absorptions correction	−	−	empirical
Max. min. transmission	−	−	0.67, 0.20
No. of variables	332	298	603
R_1, wR_2 [c]	0.039, 0.095	0.046, 0.106	0.057, 0.126

[a] Details in common: graphite monochromated radiation, refinement based on F^2. [b] Rotating anode source. [c] $R_1 = \Sigma\|\|F_o| - |F_c\|/\Sigma|F_o|$; $wR_2 = \{\Sigma[w(F_o^2 - F_c^2)^2]/\Sigma[w(F_o^2)^2]\}^{1/2}$; $w^{-1} = \sigma^2(F_o^2) + (aP)^2 + bP$.

started to loose its colour and a dark purple solid precipitated. This solid was filtered and washed several times with CH_2Cl_2 to yield *trans*-**2** as a pure compound. Yield: 0.378 g (64%). $C_{60}H_{46}Cl_2N_6O_2P_2Ru$ (1116.1): calcd. C 64.45, H 4.12, N 7.52; found C 63.92, H 4.07, N 6.94. IR (KBr): $\tilde{\nu}$ = 3342 (w) (CO−*NH*, noncoordinated carboxamide), 3048 (w) (py*H*), 1690 (vs) (CO, noncoordinated carboxamide), 1648 (vs) (CO, *N*−bound amidato group), 1604 (m), 1573 (s) (C=N); $^{31}P\{^1H\}$ NMR (CD_2Cl_2): δ = 25.5 ppm. FAB$^+$−MS: *m/z* = 1081 $[M - Cl]^+$, 783 $[Ru(L2)(PPh_3)]^+$, 521 $[Ru(L2)]^+$.

Crystallography: Table 5 provides a summary of the crystallographic data for compounds L1, L2 and **1**. Data were collected on Siemens P4 diffractometers using ω-scans. The structures were solved by direct methods and refined based on F^2 using the SHELXTL program system.[14] CCDC-191577 (for L1), -191578 (for **1**) and -191579 (for L2) contain the supplementary crystallographic data for this paper. These data can be obtained free of charge at www.ccdc.cam.ac.uk/conts/retrieving.html [or from the Cambridge Crystallographic Data Centre, 12 Union Road, Cambridge CB2 1EZ, UK; Fax: (internat.) +44-1223-336-033; E-mail: deposit@ccdc.cam.ac.uk].

Computational Details

Ab initio molecular orbital calculations on compound **1** and the *cis* and *trans* isomers of compound **2** were performed All three molecules have been subjected to geometry optimisation using density functional theory (DFT) at the B3LYP level of theory[15−17] using the 3−21G* basis set.[18] The structures were model built with no reference to the crystal structure of compound **1**. All stationary points have been characterised as minima by calculation and inspection of the vibrational modes. We have not scaled the vibrational frequencies reported in this paper. All calculations were performed with Gaussian 98.[17]

Acknowledgments

The Department of Chemistry at Imperial College is gratefully acknowledged for a Teaching Assistantship Grant (D. R.).

[1] H. Sigel, R. B. Martin, *Chem. Rev.* **1982**, *82*, 385.
[2] [2a] D. S. Marlin, P. K. Mascharak, *Chem. Soc. Rev.* **2000**, *29*, 69 and references cited therein. [2b] A. K. Patra, J. M. Rowland, D. S. Marlin, E. Bill, M. M. Olmstead, P. K. Mascharak, *Inorg. Chem.* **2003**, *42*, 6812.
[3] E. Kimura, H. Kurosaki, Y. Kurogi, M. Shionoya, M. Shiro, *Inorg. Chem.* **1992**, *31*, 4314.
[4] T. J. Collins, *Acc. Chem. Res.* **1994**, *27*, 279 and references cited therein.
[5] See for example: S. Dutta, P. K. Bhattacharya, *J. Mol Cat. A: Chem.* **2002**, *188*, 45.
[6] [6a] S. Dutta, S. Pal, P. K. Bhattacharya, *Polyhedron* **1999**, *18*, 2157. [6b] S. Dutta; P. K. Bhattacharya, E. R. T. Tiekink, *Polyhedron* **2001**, *20*, 2027. [6c] A. K. Singh, V. Balamurugan, R. Mukherjee, *Inorg. Chem.* **2003**, *42*, 6497.
[7] S. M. Redmore, C. E. F. Rickard, S. J. Webb, L. J. Wright, *Inorg. Chem.* **1997**, *36*, 4743.
[8] [8a] S.-T. Cheng, E. Doxiadi, R. Vilar, A. J. P. White, D. J. Williams, *J. Chem. Soc., Dalton Trans.* **2001**, 2239. [8b] H. A. Burkill, R. Vilar, A. J. P. White, D. J. Williams, *J. Chem. Soc., Dalton Trans.* **2002**, 837.
[9] [9a] M. S. Luth, E. Freisinger, B. Lippert, *Chem. Eur. J.* **2001**, *7*, 2104. [9b] C. R. Bondy, P. A. Gale, S. J. Loeb, *Chem. Commun.* **2001**, 729. [9c] H. Aït-Haddou, S. L. Wiskur, V. M. Lynch, E. V. Anslyn, *J. Am. Chem. Soc.* **2001**, *123*, 11296. [9d] S. Aoki, K. Iwaida, N. Hanamoto, M. Shiro, E. Kimura, *J. Am. Chem. Soc.* **2002**, *124*, 5256. [9e] J. S. Disch, R. J. Staples, T. E. Concolino, T. E. Haas, E. V. Rybak-Akimova, *Inorg. Chem.* **2003**, *42*, 6749.
[10] [10a] A. D. Burrows, C.-W. Chan, M. M. Chowdhry, J. E. McGrady, D. M. P. Mingos, *Chem. Soc. Rev.* **1995**, *24*, 329 and references cited therein. [10b] M. T. Allen, A. D. Burrows, M. F. Mahon, *J. Chem. Soc., Dalton Trans.* **1999**, 215. [10c] A. D. Burrows, D. M. P. Mingos, A. J. P. White, D. J. Williams, *J. Chem. Soc., Dalton Trans.* **1996**, 3805. [10d] L. Brammer, J. C. M. Rivas, R. Atencio, S. Y. Fang, F. C. Pigge, *J. Chem. Soc., Dalton Trans.* **2000**, 3855.
[11] Examples of biomimetic models of metallo-enzymes which use H-bonding for recognition are: [11a] K. Matsumura, M. Endo, M. Komiyama, *J. Chem. Soc., Chem. Commun.* **1994**, 2019. [11b] W. C. Putman, J. K. Bashkin, *Chem. Commun.* **2000**, 767. [11c] S. Matsuda, A. Ishikubo, A. Kuzuya, M. Yashiro, M. Komiyama, *Angew. Chem. Int. Ed.* **1998**, *37*, 3284.
[12] [12a] C. J. Chandler, L. W. Deady, J. A. Reiss, *J. Heterocyclic Chem.* **1981**, *18*, 599. [12b] P. T. Kaye, K. W. Wellington, *Synth. Commun.* **2001**, *31*, 799.
[13] A. A. Batista, M. O. Santiago, C. L. O. Donnici, I. S. Moreira, P. C. Healy, S. J. Berners-Price, S. L. Queiroz, *Polyhedron* **2001**, *20*, 2123.
[14] *SHELXTL PC* version 5.03, Siemens Analytical X-ray Instruments, Inc., In Madison, WI, **1994**; *SHELXTL PC* version 5.1, Bruker AXS, Madison, WI, **1997**.
[15] C. Lee, W. Yang, R. G. Parr, *Phys. Rev. B* **1988**, *37*, 785.
[16] B. Miehlich, A. Savin, H. Stoll, H. Preuss, *Chem. Phys. Lett.* **1989**, *157*, 200.
[17] A. D. Becke, *J. Chem. Phys.* **1993**, *98*, 5648.
[18] [18a] J. S. Binkley, J. A. Pople, W. J. Hehre, *J. Am. Chem. Soc.* **1980**, *102*, 939. [18b] M. S. Gordon, J. S. Binkley, J. A. Pople, W. J. Pietro, W. J. Hehre, *J. Am. Chem. Soc.* **1982**, *104*, 2797. [18c] W. J. Pietro, M. M. Francl, W. J. Hehre, D. J. Defress, J. A. Pople, J. S. Binkley, *J. Am. Chem. Soc.* **1982**, *104*, 5039. [18d] K. D. Dobbs, W. J. Hehre, *J. Comp. Chem.* **1986**, *7*, 359. [18e] K. D. Dobbs, W. J. Hehre, *J. Comp. Chem.* **1987**, *8*, 861. [18f] K. D. Dobbs, W. J. Hehre, *J. Comp. Chem.* **1987**, *8*, 880.
[19] Gaussian 98, Revision A.11.3, M. J. Frisch, G. W. Trucks, H. B. Schlegel, G. E. Scuseria, M. A. Robb, J. R. Cheeseman, V. G. Zakrzewski, J. A. Montgomery, Jr., R. E. Stratmann, J. C. Burant, S. Dapprich, J. M. Millam, A. D. Daniels, K. N. Kudin, M. C. Strain, O. Farkas, J. Tomasi, V. Barone, M. Cossi, R. Cammi, B. Mennucci, C. Pomelli, C. Adamo, S. Clifford, J. Ochterski, G. A. Petersson, P. Y. Ayala, Q. Cui, K. Morokuma, N. Rega, P. Salvador, J. J. Dannenberg, D. K. Malick, A. D. Rabuck, K. Raghavachari, J. B. Foresman, J. Cioslowski, J. V. Ortiz, A. G. Baboul, B. B. Stefanov, G. Liu, A. Liashenko, P. Piskorz, I. Komaromi, R. Gomperts, R. L. Martin, D. J. Fox, T. Keith, M. A. Al-Laham, C. Y. Peng, A. Nanayakkara, M. Challacombe, P. M. W. Gill, B. Johnson, W. Chen, M. W. Wong, J. L. Andres, C. Gonzalez, M. Head-Gordon, E. S. Replogle, and J. A. Pople, Gaussian Inc., Pittsburgh, PA, **2002**.

Received November 3, 2003
Early View Article
Published Online March 18, 2004

